Fractal wavelets of Dutkay-Jorgensen type for the Sierpinski gasket space

Jonas D'Andrea, Kathy D. Merrill, and Judith Packer

ABSTRACT. Several years ago, D. Dutkay and P. Jorgensen developed the concept of wavelets defined on a σ-finite fractal measure space, developed from an iterated affine system. They worked out in detail the wavelet and filter functions corresponding to the ordinary Cantor fractal subset of $\mathbb{R}$. In this paper we examine the construction of Dutkay and Jorgensen as applied to the fractal measure space corresponding to the Sierpinski gasket fractal. We develop a variety of high-pass filters, and as an application use the various families of wavelets to analyze digital photos.

1. Introduction

Two years ago, D. Dutkay and P. Jorgensen introduced the notion of multi-resolution analysis bases on σ-finite measure spaces built from dilations and translations on a fractal arising from an iterated affine function system [**DJ**]. Although their construction works in a very general setting, the details were mainly worked out in the one-dimensional setting, in particular for the ordinary Cantor set and its variants. In the case of the ordinary Cantor fractal, they used Hutchinson measure $\mathcal{H}$ on the inflated fractal measure space $\mathcal{R}$ and considered a multiresolution $L^2(\mathcal{R}, \mathcal{H})$ constructed from dilation by 3 and integer translation. The self-similarity of the Cantor set under dilation by 3 gave a polynomial variant of a low-pass filter, and using "gap-filling" and "detail" high-pass filters allowed them to construct the wavelet. In further work on the Cantor fractal case, D. Dutkay used the polynomial low-pass filter to construct a probability measure ν on the solenoid Σ_3 and a mock Fourier transform $\mathcal{F}: L^2(\mathcal{R}, \mathcal{H}) \to L^2(\Sigma_3, \nu)$, such that Fourier-transformed version of the dilation operator correpsonded to the shift automorphism on Σ_3, and the translation operator on $L^2(\mathcal{R}, \mathcal{H})$ corresponded to multiplication operators on $L^2(\Sigma_3, \nu)$ [**Dut**].

In this paper our aim is to study this construction in the case of the right triangle Sierpinski gasket. Accordingly, we let $\mathcal{S}_0$ be the points inside and on the right triangle with vertices $(0,0)$, $(0,1)$, and $(1,0)$ in $\mathbb{R}^2$. Consider the diagonal dilation matrix $A = \begin{pmatrix} 2 & 0 \\ 0 & 2 \end{pmatrix}$. Let

$$\mathcal{S}_1 = [A^{-1}(\mathcal{S}_0 + \tau_0)] \cup [A^{-1}(\mathcal{S}_0 + \tau_1)] \cup [A^{-1}(\mathcal{S}_0 + \tau_2)],$$

where $\tau_0 = (0,0)$, $\tau_1 = (1,0)$ and $\tau_2 = (0,1)$. Proceeding inductively, given $\mathcal{S}_n$, let

$$\mathcal{S}_{n+1} = [A^{-1}(\mathcal{S}_n + \tau_0)] \cup [A^{-1}(\mathcal{S}_n + \tau_1)] \cup [A^{-1}(\mathcal{S}_n + \tau_2)].$$

We thus have a nested sequence $\{\mathcal{S}_n\}_{n=0}^{\infty}$ of compact subsets of $\mathbb{R}^2$, and we define the Sierpinski gasket fractal by

$$\mathcal{S} \; = \; \cap_{n=0}^{\infty} \mathcal{S}_n.$$

The Sierpinski gasket $\mathcal{S}$ satisfies the self-similarity relation

$$A(\mathcal{S}) \; = \; \mathcal{S} \cup [\mathcal{S} + (1,0)] \cup [\mathcal{S} + (0,1)].$$

The Hausdorff dimension of $\mathcal{S}$ is known to be $s = \frac{\log 3}{\log 2}$. In the usual fashion one constructs the Hausdorff fractal measure corresponding to this dimension $\mathcal{H}^s$ on $\mathcal{S}$ ([**Hut**]), hereafter denoted by $\mathcal{H}$. Note that

$$\mathcal{H}(A^{-1}(\mathcal{S})) \; = \frac{1}{3}\mathcal{H}(\mathcal{S}) = \frac{1}{3},$$

and more generally, if E is a Borel subset of $\mathcal{S}$,

$$\mathcal{H}(A^{-1}(E)) \; = \frac{1}{3}\mathcal{H}(E).$$
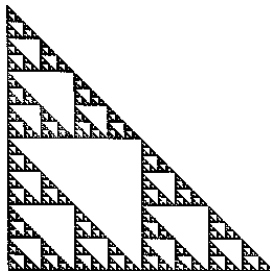
FIGURE 1. Sierpinski gasket

Just as in the Dutkay and Jorgensen work on the Cantor set, we will construct our wavelets not on the Sierpinski gasket itself, but rather on an enlarged fractal that supports a structure closer to a standard multiresolution analysis. In this respect, our work differs, for example, from Stricharz's wavelets for piecewise linear functions on triangulations of the Sierpinski gasket itself [**Str**]. In Section 2, we will describe the enlarged fractal for the Sierpinski gasket, and define the multiresolution analysis structure supported on it. In Section 3, we will use this multiresolution analysis to build a parametrized family of filters, and from them, wavelets on our space. We then go on to apply some of these wavelets to analyze digital photos in Section 4. We note that it is our use of the enlarged fractal, and thus the inclusion of "gap-filling" high-pass filters, that makes our wavelets reasonable candidates for describing images in $L^2(\mathbb{R}^2)$ rather than just on the fractal itself. The effects that using this type of wavelet has on image reconstruction will be explored further in Section 4.

2. A multiresolution analysis corresponding to the Sierpinski gasket space

We now recall the σ-finite measure space from which we obtain the dilation and translation operators to build the promised multiresolution analysis. Define the inflated fractal set $\mathcal{R}_{\mathcal{S}}$ associated to the Sierpinski gasket $\mathcal{S}$ by

$$\mathcal{R}_{\mathcal{S}} = \cup_{j=-\infty}^{\infty} \cup_{(m,n)\in\mathbb{Z}^2} [A^j(\mathcal{S} + (m,n))].$$

The probability measure $\mathcal{H}$ on $\mathcal{S}$ extends to a σ-finite measure that we also call $\mathcal{H}$ on $\mathcal{R}_{\mathcal{S}}$. This measure satisfies

$$\mathcal{H}(A^{-1}(E)) = \frac{1}{3}\mathcal{H}(E),$$

$$\mathcal{H}(E + (m,n)) = \mathcal{H}(E),$$

for every Borel subset E of $\mathcal{R}_{\mathcal{S}}$, and for every $(m,n) \in \mathbb{Z}^2$. Forming the Hilbert space $L^2(\mathcal{R}_{\mathcal{S}}, \mathcal{H})$, we can construct the unitary dilation operator D and a unitary representation of $\mathbb{Z}^2$ on $L^2(\mathcal{R}_{\mathcal{S}}, \mathcal{H})$ by

$$D(f)(s,t) = \sqrt{3}f(2s, 2t),$$

and

$$T_{(m,n)}f(s,t) = f(s - m, t - n).$$

These operators satisfy a standard commutation relation:

PROPOSITION 2.1. *Let D and $\{T_{(m,n)} : (m,n) \in \mathbb{Z}^2\}$ be the unitary operators on $L^2(\mathcal{R}_{\mathcal{S}}, \mathcal{H})$ defined above. Then*

$$T_{(m,n)}D = DT_{(2m,2n)}, \ \forall (m,n) \in \mathbb{Z}^2.$$

PROOF. This is an easy calculation. $\qquad\square$

Thus, as in the paper by the third author, L.H. Lim, and K. Taylor, the operators $\{T_{(m,n)} : (m,n) \in \mathbb{Z}^2\}$ and $\{D^j : j \in \mathbb{Z}\}$ generate a representation of the generalized Baumslag-Solitar group $\mathbb{Q}_A \ltimes \mathbb{Z}$. Here the group of generalized A-adic rationals is defined by

$$\mathbb{Q}_A = \cup_{j=0}^{\infty} A^{-j}(\mathbb{Z}^2),$$

and the automorphism of $\mathbb{Z}$ on $\mathbb{Q}_A$ corresponds to the action of matrix multiplication by integer powers of A.

We now use the dilation operator D in the standard way to construct a multiresolution analysis of the Hilbert space $L^2(\mathcal{R}_{\mathcal{S}}, \mathcal{H})$. Define a closed subspace $V_0 \subset L^2(\mathcal{R}_{\mathcal{S}}, \mathcal{H})$ by

$$V_0 = \overline{\text{span}}\{T_{(m,n)}(\chi_{\mathcal{S}}) : (m,n) \in \mathbb{Z}^2\}.$$

Here $\chi_{\mathcal{S}}$ is the characteristic function of the Sierpinski gasket triangle, and corresponds to the scaling function in the standard multi-resolution analysis set-up. The Sierpinski gasket $\mathcal{S}$ satisfies the self-similarity relation

(2.1) $$A(\mathcal{S}) = \mathcal{S} \cup [\mathcal{S} + (1,0)] \cup [\mathcal{S} + (0,1)],$$

and up to sets of measure 0, the above union is a disjoint union. It follows that its characteristic function $\chi_{\mathcal{S}}$ satisfies the dilation equation

(2.2) $$\chi_{\mathcal{S}}(A^{-1}(s,t)) = \chi_{\mathcal{S}}(s,t) + \chi_{\mathcal{S}}(s-1,t) + \chi_{\mathcal{S}}(s,t-1).$$

By construction, V_0 is invariant under the operators $\{T_{(m,n)} : (m,n) \in \mathbb{Z}^2\}$. For each $j \in \mathbb{Z}$, define

$$V_j = D^j(V_0).$$

We note that

$$\begin{aligned}
V_1 &= D(\overline{\text{span}}\{T_{(m,n)}(\chi_{\mathcal{S}}) : (m,n) \in \mathbb{Z}^2\}) \\
&= \overline{\text{span}}\{DT_{(m,n)}(\chi_{\mathcal{S}}) : (m,n) \in \mathbb{Z}^2\} \\
&= \overline{\text{span}}\{T_{(m/2,n/2)}D(\chi_{\mathcal{S}}) : (m,n) \in \mathbb{Z}^2\},
\end{aligned}$$

and consequently

$$V_0 \subseteq D(V_0) = V_1.$$

It follows that the closed subspaces $\{V_j\}_{j=-\infty}^{\infty}$ form an increasing nested sequence of closed spaces of $L^2(\mathcal{R}_{\mathcal{S}}, \mathcal{H})$.

The following result shows that the subspaces $\{V_j\}_{j=-\infty}^{\infty}$ form a multiresolution analysis. The first three items are similar in nature to Proposition 2.8 of [DJ], although the proof of item (iii) is somewhat different.

PROPOSITION 2.2. *Let* $\{V_j\}_{j=-\infty}^{\infty}$ *be the subspaces of* $L^2(\mathcal{R}_{\mathcal{S}}, \mathcal{H})$ *constructed above, and let* D, $\{T_{(m,n)} : (m,n) \in \mathbb{Z}^2\}$ *be the unitary operators constructed in Proposition 2.1. Then*

(i) $D^{-1}(\chi_{\mathcal{S}}) = \frac{1}{\sqrt{3}}[\chi_{\mathcal{S}} + T_{(1,0)}(\chi_{\mathcal{S}}) + T_{(0,1)}(\chi_{\mathcal{S}})].$

(ii) $\langle T_{(m,n)}(\chi_{\mathcal{S}}), \chi_{\mathcal{S}} \rangle = \delta_{(m,n),(0,0)}, \ (m,n) \in \mathbb{Z}^2.$

(iii) $\overline{\cup_{j=-\infty}^{\infty}[V_j]} = L^2(\mathcal{R}_{\mathcal{S}}, \mathcal{H}).$

(iv) $\cap_{j=-\infty}^{\infty}[V_j] = \{\vec{0}\}.$

PROOF. The proof of item (i) follows directly from the self-similarity relation of the Sierpinski gasket $\mathcal{S}$ and corresponding dilation equation outlined in Equations 2.1 and 2.2. Item (ii) is done by a similarly easy calculation, noting that translates of the Sierpinski gasket $\mathcal{S}$ by non-zero vectors in $\mathbb{Z}^2$ intersect $\mathcal{S}$ in sets of $\mathcal{H}$ measure 0.

As for item (iii), it will suffice to show that any Hausdorff measurable subset $E \subset \mathcal{R}_{\mathcal{S}}$ with $\mathcal{H}(E) < \infty$ has the property that χ_E is in the closure of the span of $\{D^j T_{(m,n)}(\chi_{\mathcal{S}}) \mid j, m, n \in \mathbb{Z}\}$. Since $\mathcal{R}_{\mathcal{S}} = \cup_{j=-\infty}^{\infty} \cup_{(m,n)\in\mathbb{Z}^2} [A^j(\mathcal{S} + (m,n))]$, we can write such a set $E = \cup E_{(j,m,n)}$, where $E_{(j,m,n)} = E \cap [A^j(\mathcal{S} + (m,n))]$. It is enough to show that the characteristic function of each set $E_{(j,m,n)}$ is in the closure of the span, so that by applying dilations and translations, we may without loss of generality assume that our arbitrary measurable set $E \subset \mathcal{S}$.

Let $\mathcal{V}$ be the collection of all the lower left vertices of subtriangles in S. By writing each $\{\vec{v}\} \in \mathcal{V}$ as a decreasing intersection: $\{\vec{v}\} = \cap_{n=1}^{\infty} T_n$, where each T_n is an nth dilate of a translate of $\mathcal{S}$, we see that $\mathcal{H}(\{\vec{v}\}) = \lim_{n\to\infty} \mathcal{H}(T_n) = \lim_{n\to\infty} \frac{1}{3^n} = 0$. By countable subadditivity of measures, we then have $\mathcal{H}(\mathcal{V}) = 0$. Now let $\mathcal{S}' = \mathcal{S} \sim \mathcal{V}$. Then $\mathcal{H}(\mathcal{S}') = \mathcal{H}(\mathcal{S}) = 1$. Since $\mathcal{S}$ is a metric space, so is $\mathcal{S}'$, although $\mathcal{S}'$ is no longer closed.

Thus, again without loss of generality, we assume that $E \subset \mathcal{S}'$. Let

$$\mathcal{T} = \{A^{-k}(\mathcal{S} + (i,j)) \cap \mathcal{S}' : \ k \in \mathbb{N}, \ (i,j) \in \{(0,0), \ (1,0), \ (0,1)\}\}.$$

Then $\mathcal{T}$, which consists of the "sub-Sierpinski gaskets" of $\mathcal{S}'$, is a semi-algebra of subsets of $\mathcal{S}'$; that is, finite disjoint unions of elements fromm $\mathcal{T}$ form an algebra of subsets of $\mathcal{S}'$. We denote this algebra by $\mathcal{A}$. Applying Hausdorff measure to the algebra $\mathcal{A}$, we obtain a set-valued function on $\mathcal{A}$, denoted by μ^*, which satisfies the

conditions of the Carathéodory Extension Theorem. Therefore μ^* can be extended to an outer measure on all subsets of $\mathcal{S}'$, and μ^* agrees with Hausdorff measure $\mathcal{H}$ on the algebra $\mathcal{A}$ by construction. Thus μ^* determines a σ-algebra $\mathcal{M}$ of measurable sets, which contains the smallest σ-algebra $\mathcal{B}$ containing $\mathcal{A}$. If we denote the outer measure μ^* restricted to $\mathcal{M}$, now a measure, by μ, recall that $(X, \mathcal{M}, \mu)$ is a complete measure space. Moreover, since $\mu^*(\mathcal{S}') = \mathcal{H}(\mathcal{S}')$ is finite, the Carathéodory Extension Theorem tells us this extension of $\mathcal{H}$ on $\mathcal{A}$ to the smallest σ-algebra containing $\mathcal{A}$ is unique. It follows that $\mu = \mathcal{H}$ on $\mathcal{B}$, and also on $\mathcal{M}$. The question that remains is whether or not the σ-algebra that arises when one constructs the outer Hausdorff measure on subsets of $\mathcal{S}'$, is larger than the σ-algebra $\mathcal{M}$ arising using the Carathéodory Extension Theorem with the Hausdorff measure $\mu = \mathcal{H}$.

Note that the family of sets $\mathcal{T}$, in addition to being a semi-algebra of subsets of $\mathcal{S}'$, is a Vitali cover for any subset of $\mathcal{S}'$, that is, for each $x \in E$ and each $\delta > 0$, there is a subset $T \in \mathcal{T}$ with $x \in T$ and $0 < \mathcal{H}(T) \leq \delta$. By [**Ed2**], p.10, outer measures constructed using the Carathéodory Extension Theorem from Vitali covers are metric outer measures, and so satisfy $\mu^*(A \cup B) = \mu^*(A) + \mu^*(B)$ for any subsets A and B with $d(A, B) > 0$. Furthermore, if ν^* is a metric outer measure on a metric space X, then the σ-algebra of measurable sets with respect to this outer measure contains the σ-algebra of Borel sets of X([**Ed1**], 5.2.6). We apply this result to $(\mathcal{S}', \mathcal{M}, \mu)$ to deduce that μ^* is a metric outer measure and $\mathcal{M}$ contains the Borel sets of $\mathcal{S}'$. Thus, the σ-algebra of measurable sets of $\mathcal{S}'$ constructed from μ^* contains the Borel sets of $\mathcal{S}'$ and hence the open and closed sets of $\mathcal{S}'$. It follows that $\mathcal{H}$ agrees with μ on the Borel subsets of $\mathcal{S}$.

Finally, if one constructs a finite measure μ on a set X using a algebra $\mathcal{A}$ of sets using the Carathéodory Extension Theorem, then given any measurable set $G \subset X$, there exists a element R of $\mathcal{A}$ such that $\mu(G \Delta R) < \epsilon$ by Theorem 1.1.9 of [**Ed2**].

Applying this last result to our set-up, and the measurable subset E of $\mathcal{S}'$, we note that there exists a F_σ-set $F \subset E$ with $\mathcal{H}(E \Delta F) = \mathcal{H}(E \sim F) = 0$. We then deduce that there is a finite collection of finite sub-Sierpinski gasket triangles $T_i{}^n_{i=1}$ from $\mathcal{T}$ with $\mu(F \Delta \cup^n_{i=1} T_i) < \epsilon$. Since $\mu = \mathcal{H}$ on the σ-algebra of Borel sets of $\mathcal{S}'$, $\mathcal{H}(F \Delta \cup^n_{i=1} T_i) < \epsilon$. But since $\mathcal{H}(E \Delta F) = 0$, we see that $\mathcal{H}(E \Delta \cup^n_{i=1} T_i) < \epsilon$. Thus, χ_E is in the closure of the span of $\{D^j T_{(m,n)}(\chi_\mathcal{S}) \mid j, m, n \in \mathbb{Z}\}$.

It remains to establish item (iv). Note that if $(x, y) \in \text{support}(f)$ for $f \in \cap^\infty_{j=-\infty} V_j$, then for each $j \in \mathbb{Z}$, $(x, y) \in A^j(S + (u_j, v_j))$ for some $(u_j, v_j) \in \mathbb{Z}^2$. For j large enough that $x^2 + y^2 < 2^{2j-1}$, this forces $(u_j, v_j) \in \{(0,0), (0,-1), (-1,0)\}$ and also forces (u_j, v_j) to be constant for these j. Thus, (x, y) must be in one of the nested unions $\cup^\infty_{j=-\infty} A^j \mathcal{S}$, $\cup^\infty_{j=-\infty} A^j(\mathcal{S} + (0,-1))$, or $\cup^\infty_{j=-\infty} A^j(\mathcal{S} + (-1,0))$. Since $f \in V_{-j}$ must be constant on sets of the form $A^j(\mathcal{S} + (u, v))$, the fact that each union is nested means that f must be constant on each of these unions. As the measure of each union is infinite, these constants must all be 0. $\qquad\square$

3. A parametrized family of high-pass filters for the Sierpinski gasket scaling function

Recall that in the multiresolution analysis we have constructed for $L^2(\mathcal{R}_\mathcal{S}, \mathcal{H})$,

$$V_0 = \overline{\text{span}}\{T_{(m,n)}(\chi_\mathcal{S}) : (m,n) \in \mathbb{Z}^2\},$$

and the $\{T_{(m,n)}(\chi_S)\}$ form an orthonormal basis for V_0. Thus there is the standard isometric isomorphism $J : V_0 \rightarrow L^2(\mathbb{T}^2)$ given by

$$J(\sum_{(m,n)\in\mathbb{Z}^2} c_{m,n}T_{(m,n)}(\chi_S)) = \sum_{(m,n)\in\mathbb{Z}^2} c_{m,n}e_{(m,n)},$$

where $\{c_{m,n}\} \subset l^2(\mathbb{Z})$ and $\{e_{(m,n)}(z,w) = z^m\,w^n\}$ is the standard orthonormal basis for $L^2(\mathbb{T}^2)$.

Recall $D^{-1}(V_0) = V_{-1} \subset V_0$. It follows that $J(V_{-1}) \subset L^2(\mathbb{T}^2)$, and that

$$J(V_0) = J(V_{-1} \oplus W_{-1}) = J(V_{-1}) \oplus J(W_{-1}),$$

where $W_{-1} = V_{-1}^\perp \cap V_0$. Now we calculate

$$J(D^{-1}(\chi_S)) = J(\frac{1}{\sqrt{3}}[\chi_S + T_{(1,0)}(\chi_S) + T_{(0,1)}(\chi_S)]) = \frac{1}{\sqrt{3}}[e_{(0,0)} + e_{(1,0)} + e_{(0,1)}].$$

This function is our substitute for the low-pass filter, and we denote the above function by m_0, so that

$$m_0(z,w) = \frac{1}{\sqrt{3}}[e_{(0,0)}(z,w) + e_{(1,0)}(z,w) + e_{(0,1)}(z,w)].$$

Our aim is to find functions $\{\eta_l : l = 1,2,3\} \subset W_{-1}$ such that $\{T_{(2m,2n)}(\eta_l) : l = 1,2,3, (m,n) \in \mathbb{Z}^2\}$ form an orthonormal basis for W_{-1}. Note that $W_0 = D(W_{-1})$. Applying D and using the commutation relation $T_{(m,n)}D = DT_{(2m,2n)}$, the functions $\psi_k = D(\eta_k)$ will be our wavelet family for $L^2(\mathcal{R}_S, \mathcal{H})$, since it will then follow that

$$\cup_{l=1}^3 \{T_{(m,n)}(\psi_l) : (m,n) \in \mathbb{Z}^2\} = \cup_{l=1}^3 \{DT_{(2m,2n)}(\eta_l) : (m,n) \in \mathbb{Z}^2\}$$

will give an orthonormal basis for W_0.

Using the fact that J is a unitary isomorphism from the Hilbert space W_{-1} into $L^2(\mathbb{T})$, we let $m_l = J(\eta_l)$, $l = 1,2,3$. Part of the problem then comes down to computing when

$$\{z^{2m}w^{2n}m_l(z,w) : (m,n) \in \mathbb{Z}^2\}$$

is an orthonormal set in $L^2(\mathbb{T}^2)$.

LEMMA 3.1. *Let f be an element of $L^2(\mathbb{T}^2)$. Then the collection of functions $\{z^{2m}w^{2n}f : (m,n) \in \mathbb{Z}^2\}$ forms an orthonormal set in $L^2(\mathbb{T}^2)$ if and only if*

$$\sum_{j=0}^1 \sum_{k=0}^1 |f(ze^{\pi ij}, we^{\pi ik})|^2 = 4.$$

PROOF. The proof comes down to a simple calculation involving Fourier coefficients and the inner products $\langle f, z^{2m}w^{2n}f \rangle$, $(m,n) \in \mathbb{Z}^2$, which we leave to the reader. □

LEMMA 3.2. *Suppose that f is as in Lemma 3.1. Then a function $g \in L^2(\mathbb{T}^2)$ is orthogonal to every function $z^{2m}w^{2n}f$ if and only if*

$$\sum_{j=0}^1 \sum_{k=0}^1 f(ze^{\pi ij}, we^{\pi ik})\overline{g(ze^{\pi ij}, we^{\pi ik})} = 0, \text{ a.e. on } \mathbb{T}^2.$$

PROOF. Again the proof involves calculations of Fourier coefficients and inner products defined by integrals, and is left to the reader. □

This leads us to the following result, which summarizes a special case of results from [**BCM02**].

PROPOSITION 3.3. *(c.f.* [**BCM02**]*) Let* $m_0 = \frac{1}{\sqrt{3}}[e_{(0,0)} + e_{(1,0)} + e_{(0,1)}]$ *be the "mutant" low-pass filter on* $\mathbb{T}^2$ *defined earlier, and let* $m_1, m_2, m_3 \in L^2(\mathbb{T}^2)$. *Then* $\{\psi_l = D(J^{-1}(m_l) : l = 1, 2, 3\}$ *is a wavelet family for* $L^2(\mathcal{R}_\mathcal{S}, \mathcal{H})$ *if and only if the functions* $\{m_l\}$ *satisfy:*

$$(3.1) \qquad \sum_{j=0}^{1}\sum_{k=0}^{1} |m_l(ze^{\pi ij}, we^{\pi ik})|^2 = 4 \ a.e. \ on \ \mathbb{T}^2.$$

$$(3.2) \qquad \sum_{j=0}^{1}\sum_{k=0}^{1} m_l(ze^{\pi ij}, we^{\pi ik})\overline{m_{l'}(ze^{\pi ij}, we^{\pi ik})} = 0, \ l \neq l',$$

and

$$(3.3) \qquad \sum_{j=0}^{1}\sum_{k=0}^{1} m_0(ze^{\pi ij}, we^{\pi ik})\overline{m_l(ze^{\pi ij}, we^{\pi ik})} = 0, \ l = 1, 2, 3.$$

We now use a proposition based in linear algebra that has been used to create polynomial high-pass filters from polynomial low-pass filters as far back as 1992, by R. Gopinath and C. Burrus [**GB**].

THEOREM 3.4. *(c.f.* [**GB**]*) Let* $\vec{v}_0 = (\frac{1}{\sqrt{3}}, \frac{1}{\sqrt{3}}, \frac{1}{\sqrt{3}}, 0), \vec{v}_1 = (a_{(0,0)}, a_{(1,0)}, a_{(0,1)}, a_{(1,1)})$, $\vec{v}_2 = (b_{(0,0)}, b_{(1,0)}, b_{(0,1)}, b_{(1,1)})$ *and* $\vec{v}_3 = (c_{(0,0)}, c_{(1,0)}, c_{(0,1)}, c_{(1,1)})$ *be vectors in* $\mathbb{C}^4$ *such that* $\{\vec{v}_0, \vec{v}_1, \vec{v}_2, \vec{v}_3\}$ *forms an orthonormal basis for* $\mathbb{C}^4$. *Then setting*

$$m_1 = \sum_{j=0}^{2}\sum_{k=0}^{2} a_{(j,k)}e_{(j,k)},$$

$$m_2 = \sum_{j=0}^{2}\sum_{k=0}^{2} b_{(j,k)}e_{(j,k)},$$

and

$$m_3 = \sum_{j=0}^{2}\sum_{k=0}^{2} c_{(j,k)}e_{(j,k)},$$

the functions $m_1, m_2,$ *and* m_3 *satisfy Equations 3.1, 3.2, and 3.3 with respect to* m_0, *so that* $\{\psi_l = D(J^{-1}(m_l)) : l = 1, 2, 3\}$ *is a wavelet family for* $L^2(\mathcal{R}_\mathcal{S}, \mathcal{H})$.

PROOF. Since the set $\{\vec{v}_0, \vec{v}_1, \vec{v}_2, \vec{v}_3\}$ forms an orthonormal basis for $\mathbb{C}^4$, the 4×4 matrix

$$M = \begin{pmatrix} 1/\sqrt{3} & 1/\sqrt{3} & 1/\sqrt{3} & 0 \\ a_{(0,0)} & a_{(1,0)} & a_{(0,1)} & a_{(1,1)} \\ b_{(0,0)} & b_{(1,0)} & b_{(0,1)} & b_{(1,1)} \\ c_{(0,0)} & c_{(1,0)} & c_{(0,1)} & c_{(1,1)} \end{pmatrix}$$

is unitary, as its rows form an orthonormal set. For $z = e^{2\pi is}$ and $w = e^{2\pi it}$, let $\vec{v}(z, w)$ denote the row vector consisting of the following functions from $C(\mathbb{T}^2)$: $(e_{(0,0)}, e_{(1,0)}, e_{(0,1)}, e_{(1,1)})$. Now note that $m_l(t) = \vec{v}_l \cdot \vec{v}(z, w), \ l = 0, 1, 2, 3.$ where

the "·" denotes dot product. We first verify that Equation 3.1 holds for m_1; the proof for m_2 and m_3 will be identical.

$$\sum_{j=0}^{1}\sum_{k=0}^{1}|m_1(ze^{\pi ij},we^{\pi ik})|^2 \; =$$

$$= \; \sum_{j=0}^{1}\sum_{k=0}^{1}(a_{(0,0)}+a_{(1,0)}ze^{\pi ij}+a_{(0,1)}we^{\pi ik}+a_{(1,1)}zwe^{\pi i(j+k)})$$

$$\overline{(a_{(0,0)}+a_{(1,0)}ze^{\pi ij}+a_{(0,1)}we^{\pi ik}+a_{(1,1)}zwe^{\pi i(j+k)})}$$

$$= \; 4|a_{(0,0)}|^2+a_{(0,0)}[\overline{a_{(1,0)}z}\sum_{j=0}^{1}\sum_{k=0}^{1}e^{-\pi ij}+\overline{a_{(0,1)}w}\sum_{j=0}^{1}\sum_{k=0}^{1}e^{-\pi ik}+\overline{a_{(1,1)}zw}\sum_{j=0}^{1}\sum_{k=0}^{1}e^{-\pi i(j+k)}]$$

$$+4|a_{(1,0)}|^2+a_{(1,0)}z[\overline{a_{(0,0)}}\sum_{j=0}^{1}\sum_{k=0}^{1}e^{\pi ij}+\overline{a_{(0,1)}w}\sum_{j=0}^{1}\sum_{k=0}^{1}e^{\pi i(j-k)}+\overline{a_{(1,1)}zw}\sum_{j=0}^{1}\sum_{k=0}^{1}e^{-\pi ik}]$$

$$+4|a_{(0,1)}|^2+a_{(0,1)}w[\overline{a_{(0,0)}}\sum_{j=0}^{1}\sum_{k=0}^{1}e^{\pi ik}+\overline{a_{(1,0)}z}\sum_{j=0}^{1}\sum_{k=0}^{1}e^{\pi i(k-j)}+\overline{a_{(1,1)}zw}\sum_{j=0}^{1}\sum_{k=0}^{1}e^{-\pi ij}]$$

$$+4|a_{(1,1)}|^2+a_{(1,1)}zw[\overline{a_{(0,0)}}\sum_{j=0}^{1}\sum_{k=0}^{1}e^{\pi i(j+k)}+\overline{a_{(1,0)}z}\sum_{j=0}^{1}\sum_{k=0}^{1}e^{-\pi ik}+\overline{a_{(0,1)}w}\sum_{j=0}^{1}\sum_{k=0}^{1}e^{-\pi ij}].$$

Repeatedly using the trivial equality

$$(3.4) \qquad\qquad \sum_{j=0}^{1}e^{\pm\pi ij}=0,$$

we see that

$$\sum_{j=0}^{1}\sum_{k=0}^{1}|m_1(ze^{\pi ij},we^{\pi ik})|^2 \; = \; 4|a_{(0,0)}|^2+4|a_{(1,0)}|^2+4|a_{(0,1)}|^2+4|a_{(1,1)}|^2=4.$$

With this and the identical calculations for m_2 and m_3, we have established Equation 3.1.

The proofs of the other two equations make similar use of 3.4. For example, to establish the $l=1$ case of Equation 3.3 we calculate that

$$\sum_{j=0}^{1}\sum_{k=0}^{1}m_0(ze^{\pi ij},we^{\pi ik})\overline{m_1(ze^{\pi ij},we^{\pi ik})}$$

$$= \sum_{j=0}^{1}\sum_{k=0}^{1}(\frac{1}{\sqrt{3}}+\frac{1}{\sqrt{3}}ze^{\pi ij}+\frac{1}{\sqrt{3}}we^{\pi ik})\overline{(a_{(0,0)}+a_{(1,0)}ze^{\pi ij}+a_{(0,1)}we^{\pi ik}+a_{(1,1)}zwe^{\pi i(j+k)})}$$

$$= \; 4\frac{1}{\sqrt{3}}\overline{a_{(0,0)}}+4\frac{1}{\sqrt{3}}\overline{a_{(1,0)}}+4\frac{1}{\sqrt{3}}\overline{a_{(1,0)}}$$

$$= \; 4\vec{v}_0\cdot\overline{\vec{v}_1} \; = \; 0.$$

We leave the remainder of the details to the reader.   □

It follows from the above theorem that modulo permuting the wavelets, one can parametrize wavelet bases corresponding to the scaling function $\chi_{\mathcal{S}}$ by ordered families of orthonormal bases for the orthogonal complement of $\{(\frac{1}{\sqrt{3}}, \frac{1}{\sqrt{3}}, \frac{1}{\sqrt{3}}, 0)\}$ in $\mathbb{R}^4$, or in $\mathbb{C}^4$ if we include complex linear combinations of dilates and translates of $\chi_{\mathcal{S}}$ as our wavelets. These correspond to a parametrization by $O(3, \mathbb{R})$ or by $U(3, \mathbb{C})$, respectively. We thus have a concrete way to construct high-pass filters associated to m_0, and we now give some examples corresponding to the case where $\vec{v}_1 = (0, 0, 0, 1)$.

EXAMPLE 3.5. Let $\vec{v}_1 = (a_{(0,0)}, a_{(1,0)}, a_{(0,1)}, a_{(1,1)}) = (0, 0, 0, 1)$; then the associated filter function is

$$m_1(z, w) \;=\; zw.$$

This corresponds to the "gap-filling wavelet" in the discussion of the Cantor set wavelets given in [**DJ**].

For this choice of m_1, we now give a family of high-pass filters $\{m_2, m_3\}$ parametrized by a circle. We first need to find unit vectors $\vec{v}_2 = (b_{(0,0)}, b_{(1,0)}, b_{(0,1)}, 0)$ and $\vec{v}_3 = (c_{(0,0)}, c_{(1,0)}, c_{(0,1)}, 0)$ that are orthogonal to $\vec{v}_0 = (\frac{1}{\sqrt{3}}, \frac{1}{\sqrt{3}}, \frac{1}{\sqrt{3}}, 0)$ and to one another. If we just want real coefficients for our polynomials, this corresponds to finding (x, y, z) with $x^2 + y^2 + z^2 = 1$ and $\frac{1}{\sqrt{3}}x + \frac{1}{\sqrt{3}}y + \frac{1}{\sqrt{3}}z = 0$, i.e. $x + y + z = 0$. The plane $x + y + z = 0$ intersects the sphere $x^2 + y^2 + z^2 = 1$ in a circle. So suppose we have $(x, y, (-x - y))$ with $x^2 + y^2 + xy = \frac{1}{2}$. Let $\vec{v}_2 = (x, y, (-x - y), 0) = (b_{(0,0)}, b_{(1,0)}, b_{(0,1)}, 0)$. Then there will be a two choices of $\vec{v}_3 = (c_{(0,0)}, c_{(1,0)}, c_{(0,1)}, 0)$ lying on the desired circle (hence a unit vector that is perpendicular to $\vec{v}_1$ and is also perpendicular to $\vec{v}_2$. The vectors $\vec{v}_2$ and $\vec{v}_3$ correspond to the detail wavelets. We see these are parametrized by the Cartesian product of the circle formed from the intersection of the sphere $x^2 + y^2 + z^2 = 1$ and the plane $x + y + z = 0$ and the two point space $\{1, -1\}$.

We parametrize the family of possible $\{\vec{v}_2\}$ by using the angular variable θ : We can have

$$\vec{v}_2 \;=\; \frac{1}{\sqrt{2 + \sin 2\theta}} (\cos\theta, \sin\theta, -\sqrt{2}\sin(\theta + \frac{\pi}{4}), 0), \; \theta \in [-\pi, \pi).$$

For each choice of $\vec{v}_2$, we have two possible choices of $\vec{v}_3$: one continuously parametrized choice is

$$\vec{v}_3 \;=\; \frac{1}{\sqrt{6 + 3\sin 2\theta}} (\sqrt{5}\sin(\theta + \alpha), -\sqrt{5}\cos(\theta - \alpha), \sqrt{2}\cos(\theta + \frac{\pi}{4}), 0),$$

for $\theta \in [-\pi, \pi)$, and where $\alpha = \arcsin\frac{1}{\sqrt{5}}$. Then

$$m_2(z, w) = \vec{v_2} \cdot (e_{(0,0)}, e_{(1,0)}, e_{(0,1)}, e_{(1,1)}) = \frac{\cos\theta + \sin\theta z - \sqrt{2}\sin(\theta + \frac{\pi}{4})w}{\sqrt{2 + \sin 2\theta}},$$

and

$$m_3(z, w) \;=\; c_{(0,0)} + c_{(1,0)}z + c_{(0,1)}w,$$

where $c_{(0,0)}, c_{(1,0)}$ and $c_{(0,1)}$ are the components of $\vec{v}_3$ parametrized above. For example, taking $\theta = -\frac{\pi}{4}$, we would have $m_2(z, w) = \frac{1}{\sqrt{2}} - \frac{1}{\sqrt{2}}z$ corresponding to the choice of vector $\vec{v}_2 = (\frac{1}{\sqrt{2}}, -\frac{1}{\sqrt{2}}, 0, 0)$. Then the possible choices of $\vec{v_3}$ are

$\vec{v}_3 = (\frac{-1}{\sqrt{6}}, \frac{-1}{\sqrt{6}}, \frac{2}{\sqrt{6}}, 0)$, (corresponding to the parametrization given by θ above) or
$\vec{v}_3 = (\frac{1}{\sqrt{6}}, \frac{1}{\sqrt{6}}, \frac{-2}{\sqrt{6}}, 0)$. In the first case we have

$$m_3(z, w) = -\frac{1}{\sqrt{6}} - \frac{z}{\sqrt{6}} + \frac{2w}{\sqrt{6}}.$$

In the second case we have

$$m_3(z, w) = \frac{1}{\sqrt{6}} + \frac{z}{\sqrt{6}} - \frac{2w}{\sqrt{6}}.$$

Our wavelet family for the first choice of m_3 is given by $\psi_i = D(J^{-1}(m_i))$ so
that

$$\psi_1 = D(T_{(1,1)}\chi_{\mathcal{S}}),$$

$$\psi_2 = \frac{1}{\sqrt{2}}D(\chi_{\mathcal{S}} - T_{(1,0)}\chi_{\mathcal{S}}),$$

$$\psi_3 = \frac{1}{\sqrt{6}}D(-\chi_{\mathcal{S}} - T_{(1,0)}\chi_{\mathcal{S}} + 2T_{(0,1)}\chi_{\mathcal{S}}).$$
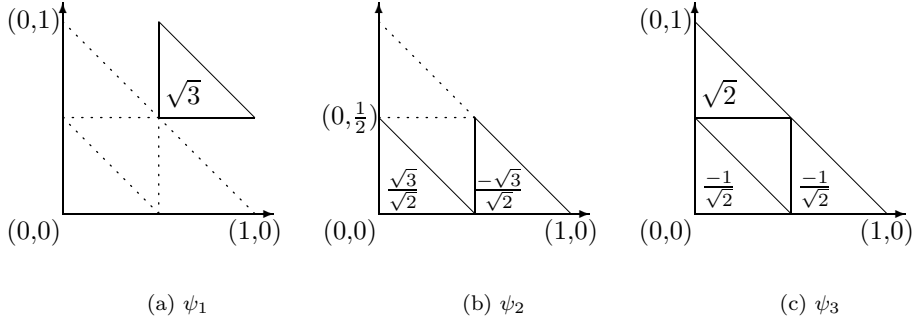
FIGURE 2. Wavelets of Example 3.5

The right triangles in the graphs of Figure 2 represent the sub-Sierpinski gaskets
obtained by dilation of $\chi_{\mathcal{S}}$ and associated translates in the construction of ψ_i.

EXAMPLE 3.6. (The D'Andrea Code) We now do an example with complex
coefficients. It has the benefit that the non-zero coefficients in the $\vec{v}_2$ and $\vec{v}_3$ have
the same modulus, thus giving a certain symmetry to the detail wavelets. This
cannot be achieved in the parametrization with real coefficients given above. We
still take $m_1(z) = zw$ corresponding to the gap-filling wavelet but for the choice of
detail wavelets we use complex coefficients for the $\vec{v}_i$, $i = 2, 3$. In particular, setting
$\lambda = e^{\frac{2\pi i}{3}}$ we let

$$\vec{v}_2 = (\frac{1}{\sqrt{3}}, \frac{\lambda}{\sqrt{3}}, \frac{\lambda^2}{\sqrt{3}}, 0)$$

and

$$\vec{v}_3 = (\frac{1}{\sqrt{3}}, \frac{\lambda^2}{\sqrt{3}}, \frac{\lambda}{\sqrt{3}}, 0),$$

and check that the hypotheses of Theorem 3.4 hold.

In this case, we get

$$m_1(z, w) \;=\; zw, \; m_2(z, w) \;=\; \frac{1}{\sqrt{3}}[1 + \lambda z + \lambda^2 w],$$

and

$$m_3(z, w) \;=\; \frac{1}{\sqrt{3}}[1 + \lambda^2 z + \lambda w],$$

so that the wavelet family is given by

$$\psi_1 \;=\; D(T_{(1,1)}\chi_{\mathcal{S}}),$$

$$\psi_2 \;=\; \frac{1}{\sqrt{3}}D(\chi_{\mathcal{S}} + \lambda T_{(1,0)}\chi_{\mathcal{S}} + \lambda^2 T_{(0,1)}\chi_{\mathcal{S}})$$

and

$$\psi_3 \;=\; \frac{1}{\sqrt{3}}D(\chi_{\mathcal{S}} + \lambda^2 T_{(1,0)}\chi_{\mathcal{S}} + \lambda T_{(0,1)}\chi_{\mathcal{S}}).$$

(a) ψ_1 (b) ψ_2 (c) ψ_3
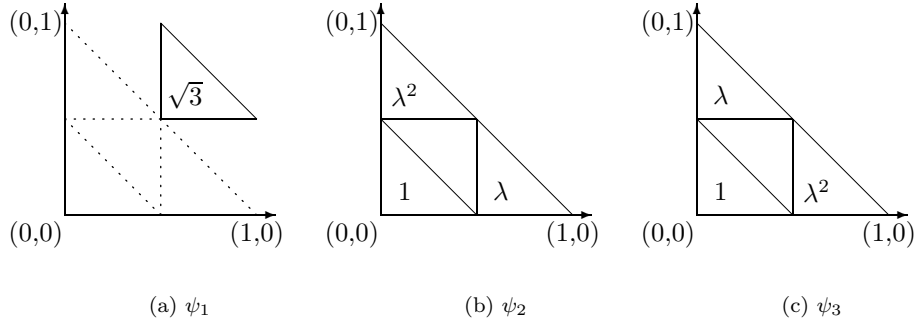
FIGURE 3. Wavelets of Example 3.6

4. Discrete Sierpinski gasket wavelet transform and image compression

In this section we will describe a discrete fractal wavelet transform based on the Sierpinski gasket space, using the filters of Examples 3.5 and 3.6. We will then apply this transform to images in $L^2(\mathbb{R}^2)$, and analyze how the results compare to those using the Haar wavelet, which is also discontinuous. For our Sierpinski gasket wavelet transform (DSGWT), we will use the same algorithm as the discrete Haar wavelet transform (DHWT), altering only the low and high-pass filters which are used. Thus, we begin by briefly describing the Haar wavelet and the DHWT.

The Haar scaling function and wavelet on $L^2(\mathbb{R}^2)$ are given by

$$\varphi \;=\; \chi_{\mathcal{Q}},$$

$$\psi_1 \;=\; \frac{1}{2}D(T_{(0,0)}\chi_{\mathcal{Q}} + T_{(1,0)}\chi_{\mathcal{Q}} - T_{(0,1)}\chi_{\mathcal{Q}} - T_{(1,1)}\chi_{\mathcal{Q}}),$$

$$\psi_2 \;=\; \frac{1}{2}D(T_{(0,0)}\chi_{\mathcal{Q}} - T_{(1,0)}\chi_{\mathcal{Q}} + T_{(0,1)}\chi_{\mathcal{Q}} - T_{(1,1)}\chi_{\mathcal{Q}}),$$

$$\psi_3 \;=\; \frac{1}{2}D(T_{(0,0)}\chi_{\mathcal{Q}} - T_{(1,0)}\chi_{\mathcal{Q}} - T_{(0,1)}\chi_{\mathcal{Q}} + T_{(1,1)}\chi_{\mathcal{Q}}),$$

where $\mathcal{Q} = [0,1) \times [0,1)$, and where

$$D(f)(s,t) \;=\; 2f(2s, 2t),$$

and

$$T_{(m,n)}f(s,t) \;=\; f(s-m, t-n)$$

are the unitary operators on $L^2(\mathbb{R}^2)$ analogous to the operators of the same name that were defined in Section 2 on $L^2(\mathcal{R}_\mathcal{S}, \mathcal{H})$.

(a) ψ_1 (b) ψ_2 (c) ψ_3
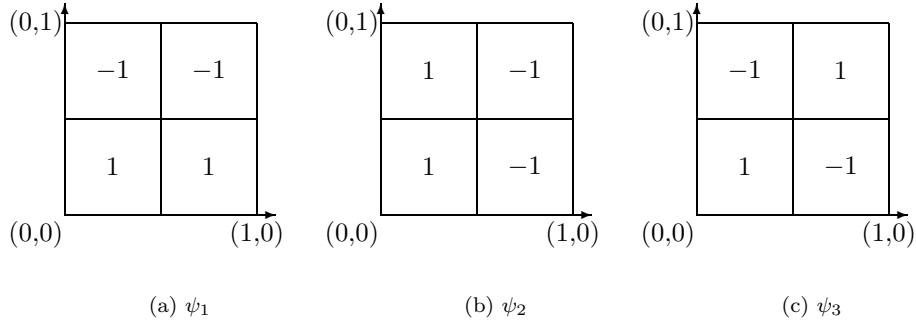
FIGURE 4. Haar wavelets on $L^2(\mathbb{R}^2)$

The scaling function φ defines a multiresolution analysis of $L^2(\mathbb{R}^2)$ in the usual way with

$$V_j \;=\; \overline{\operatorname{span}}\{D^j T_{(m,n)}(\varphi) : (m,n) \in \mathbb{Z}^2\}.$$

Also in the usual way, if we let W_j be defined by $V_{j+1} \;=\; V_j \oplus W_j$, then

$$\cup_{i=1}^3 \{D^j T_{(m,n)}(\psi_i) : (m,n) \in \mathbb{Z}^2\}$$

forms an orthonormal basis of W_j.

The Haar scaling function and wavelet can be constructed from filters which can in turn be described by unit vectors in $\mathbb{R}^4$ in a similar fashion to the Sierpinski wavelets of the previous section. The Haar low-pass filter is described by the unit vector,

$$\vec{v}_0 \;=\; (\frac{1}{2}, \frac{1}{2}, \frac{1}{2}, \frac{1}{2}),$$

and high-pass filters by the unit vectors

$$\vec{v}_1 \;=\; (\frac{1}{2}, \frac{1}{2}, \frac{-1}{2}, \frac{-1}{2}),$$

$$\vec{v}_2 \;=\; (\frac{1}{2}, \frac{-1}{2}, \frac{1}{2}, \frac{-1}{2}),$$

and

$$\vec{v}_3 \;=\; (\frac{1}{2}, \frac{-1}{2}, \frac{-1}{2}, \frac{1}{2}).$$

We consider a $2^n \times 2^n$ pixel grayscale image, supported on the unit square, as a function in V_n, and represent it by a $2^n \times 2^n$ matrix B whose entries are intensity

$2^n \times 2^n$ grayscale matrix B Transform coefficient matrix C
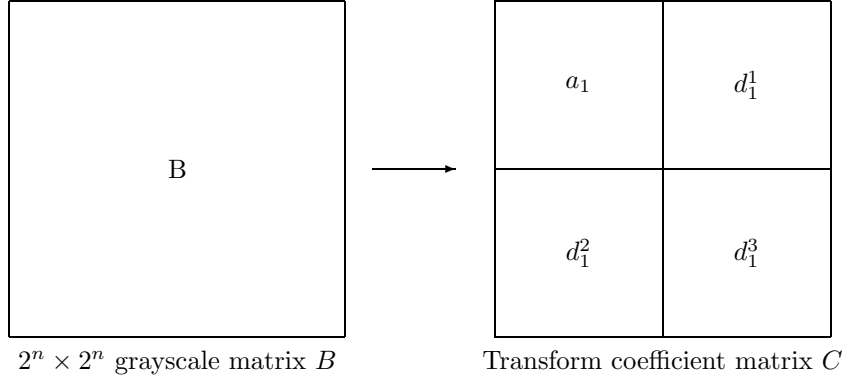
FIGURE 5. representation of 2×2 sub-matrix decomposition

values. The DHWT allows us to decompose B in the following manner. We take a 2×2 sub-matrix of B and write it as a column vector,

$$
\begin{pmatrix} b_{i,j} & b_{i,j+1} \\ b_{i+1,j} & b_{i+1,j+1} \end{pmatrix} \simeq \begin{pmatrix} b_{i+1,j} \\ b_{i+1,j+1} \\ b_{i,j} \\ b_{i,j+1} \end{pmatrix} = \vec{b}_{ij}.
$$

Multiplication by the matrix M, whose rows are the filters $\vec{v}_0, \vec{v}_1, \vec{v}_2$, and $\vec{v}_3$ (as in the proof of Theorem 3.4), yields the column vector,

$$
\vec{c}_{ij} = M\vec{b}_{ij} = \begin{pmatrix} \vec{v}_0 \\ \vec{v}_1 \\ \vec{v}_2 \\ \vec{v}_3 \end{pmatrix} \vec{b}_{ij} = \begin{pmatrix} a_{\frac{i+1}{2}, \frac{j+1}{2}} \\ d^1_{\frac{i+1}{2}, \frac{j+1}{2}} \\ d^2_{\frac{i+1}{2}, \frac{j+1}{2}} \\ d^3_{\frac{i+1}{2}, \frac{j+1}{2}} \end{pmatrix},
$$

whose entries are transform coefficients a, d^1, d^2, and d^3 which are stored in the matrix C. Since B was chosen to be a $2^n \times 2^n$ matrix, the indices (i,j) on $\vec{b}$ and $\vec{c}$ are always both odd. The indices on the entries of $\vec{c}$ are the positions of these values in the $2^{n-1} \times 2^{n-1}$ sub-matrices of C of the same name depicted in Figure 5. Hence, transform coefficients, corresponding to an original 2×2 block in B, have the same relative position in their respective sub-matrix of C, (either a_1, d^1_1, d^2_1, or d^3_1,) as the position of the original 2×2 block in B.

This describes a standard algorithm for computing the transform coefficients in a discrete setting based on the Haar wavelet family using nothing more than matrix multiplication. If we renormalize the unit square to a $2^n \times 2^n$ matrix of pixels and note that the matrix uses column information for the x shift and row information for the y shift, then the transform coefficients correspond to standard inner products in $L^2(\mathbb{R}^2)$ given by,

$$
a_{\frac{i+1}{2}, \frac{j+1}{2}} = \langle f, D^{n-1} T_{(\frac{j-1}{2}, 2^{n-1} - \frac{i+1}{2})}(\varphi) \rangle,
$$

$$
d^1_{\frac{i+1}{2}, \frac{j+1}{2}} = \langle f, D^{n-1} T_{(\frac{j-1}{2}, 2^{n-1} - \frac{i+1}{2})}(\psi_1) \rangle,
$$

$$
d^2_{\frac{i+1}{2}, \frac{j+1}{2}} = \langle f, D^{n-1} T_{(\frac{j-1}{2}, 2^{n-1} - \frac{i+1}{2})}(\psi_2) \rangle,
$$

and
$$d^3_{\frac{i+1}{2},\frac{j+1}{2}} \;=\; \langle f, D^{n-1}T_{(\frac{j-1}{2},2^{n-1}-\frac{i+1}{2})}(\psi_3)\rangle.$$

Note that these are the coefficients of the basis functions in the decomposition of
$$f \in V_n \;=\; V_{n-1} \oplus W_{n-1}$$

on the support of f corresponding to the original 2×2 block in B. Hence,
$$f_{|_E} \;=\; D^{n-1}T_{(\frac{j-1}{2},2^{n-1}-\frac{i+1}{2})}(a\varphi + d^1\psi_1 + d^2\psi_2 + d^3\psi_3),$$

where E is the support of the original 2×2 block in B, (we have suppressed the indices on the coefficients a, d^1, d^2, and d^3). In this manner we decompose B into C, which consists of the sub-matrices a_1, d^1_1, d^2_1, and d^3_1, as shown in Figure 5 (with the subscripts indicating that we have performed one level of decomposition).

(a) 2-Level decomposition

(b) Haar filter

(c) Filter of Example 3.5

(d) Filter of Example 3.6
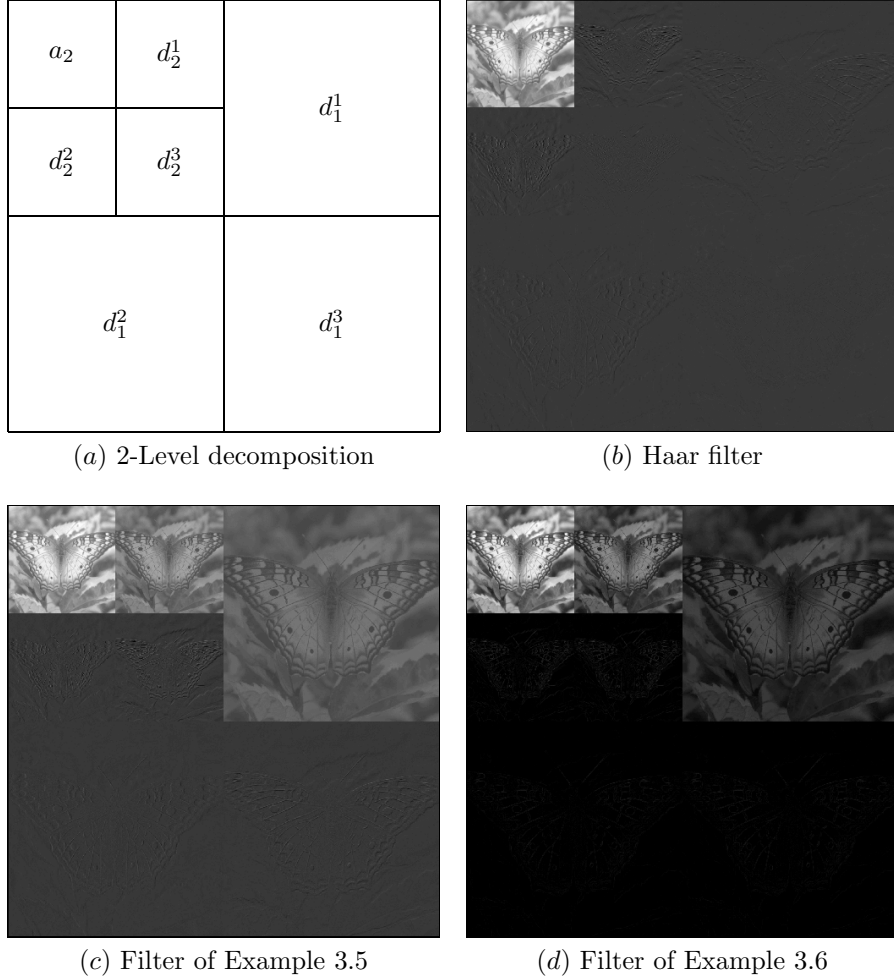
FIGURE 6. (a) 2-level coefficient decomposition scheme; (b)-(d) decomposed butterfly using various filters.

We can continue decomposing f by transforming the sub-matrix a_1 of C, achieving a second level of decomposition shown in Figure 6. This is analogous again to the decomposition of V_n as seen by

$$V_n \ = \ V_{n-2} \oplus W_{n-2} \oplus W_{n-1}.$$

Note that in this case, the entries in a_2 are the coefficients of the basis elements of V_{n-2} for this representation of f. The entries of the detail matrices $d_2^k, k = 1, 2, 3$, are the coefficients of the basis elements of W_{n-2} corresponding to the appropriate translation and dilation of ψ_k respectively for this representation of f. Similarly, $d_1^k, k = 1, 2, 3$, correspond to W_{n-1}. Since $f \in V_n$, we can perform n such decompositions by successive iterations on V_j for $j = 1, ..., n$ yielding,

$$V_n \ = \ V_0 \oplus (\oplus_{j=0}^{n-1} W_j).$$

Note that the sub-matrix a_n consists of a single entry, which is the coefficient of φ. For further details regarding the Haar wavelet family and its discrete wavelet transform see [**Mal99**].

We have detailed the DHWT because of its familiarity and because the algorithm and theory just described are essentially the same for the DSGWT. We need only change the filters, $\vec{v}_i$ for $i = 0, 1, 2, 3$, to those described in Section 3. Recall that for Examples 3.5 and 3.6 this means that $\vec{v}_0 \ = \ (\frac{1}{\sqrt{3}}, \frac{1}{\sqrt{3}}, \frac{1}{\sqrt{3}}, 0)$ and $\vec{v}_1 \ = \ (0, 0, 0, 1)$. If we consider our matrix B as the discretization of a function $f \in L^2(\mathcal{R}_\mathcal{S}, \mathcal{H})$, then this approximation to f lives in V_n of the multiresolution on $L^2(\mathcal{R}_\mathcal{S}, \mathcal{H})$ described in Section 2, and everything we just said about the DHWT still applies to the DSGWT substituting $L^2(\mathcal{R}_\mathcal{S}, \mathcal{H})$ in place of $L^2(\mathbb{R}^2)$. If however we keep B as the discretization of a function $f \in L^2(\mathbb{R}^2)$ there is nothing preventing us from using the DSGWT to decompose f. Essentially, we are then treating level n Sierpinski gaskets as pixels. Since the transform relies on the fact that M is unitary we are just reorganizing the information provided in B into a new coefficient matrix C. But now our coefficients no longer match up nicely to the standard inner product on $L^2(\mathbb{R}^2)$ of f with the appropriate basis elements since the measures on $\mathcal{R}_\mathcal{S}$ and $\mathbb{R}^2$ are different, i.e., if the unit square $\mathcal{Q} \in \mathbb{R}^2$ is represented by a 2×2 matrix then a single entry of this matrix corresponds to an area of $\frac{1}{4}$ under the $\mathbb{R}^2$ Lebesgue measure whereas a single entry of this matrix under the fractal measure $\mathcal{H}$ corresponds to an area of $\frac{1}{3}$ since it is one-third of the discretized unit Sierpinski gasket. This technicality does not affect the implementation of the DSGWT on a given matrix regardless of one's point of view.

Figure 6 shows two levels of decomposition of a 512×512 grayscale image (butterfly of Figure 7a) into transform coefficient matrices, which have also been visualized as grayscale images. These transform matrices illustrate the desirability of using certain wavelets in image compression. Grayscale intensity values take on values between zero (black) and one (white). The large amounts of black or near black areas of these transform matrices are entries which are nearly zero. Transforming the image at different levels amounts to reorganizing the information of the image with respect to the basis functions of our multiresolution analysis. Under this reorganization, energy is concentrated in the transform coefficients where the structure of the image is well-represented by the structure of the basis functions at a particular level of resolution. Thresholding or quantizing the transform matrices zeros out a certain number of entries. As long the entries being zeroed out are near zero, we are only throwing away a small amount of the information contained in

the transform matrix, and a reasonable reconstruction of the original image can
be obtained. Sparse matrices are easily compressed using various coding schemes
which we do not discuss here. So, if we can represent an image efficiently by basis
functions of a multiresolution analysis, this representation will admit a sparse ma-
trix under thresholding which contains most of the original information and can be
compressed easily. Again, we are taking advantage of image structure being similar
to basis function structure at different levels of resolution.

(a) Original

(b) Haar filter

(c) Filter of Example 3.5

(d) Filter of Example 3.6

FIGURE 7. (a) Original 512×512 grayscale image; (b)-(d) recon-
struction using 3% of transform coefficients

Reconstruction of an image from its transform coefficients is accomplished via
an inverse wavelet transform. For our examples this amounts to the matrix multi-
plication,

$$M^* \vec{c} \; = \; M^* M \vec{b} \; = \; \vec{b},$$
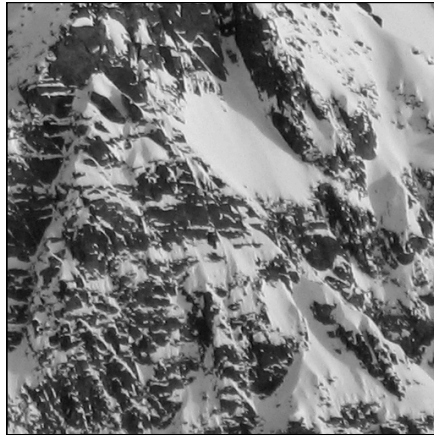
(a) Original
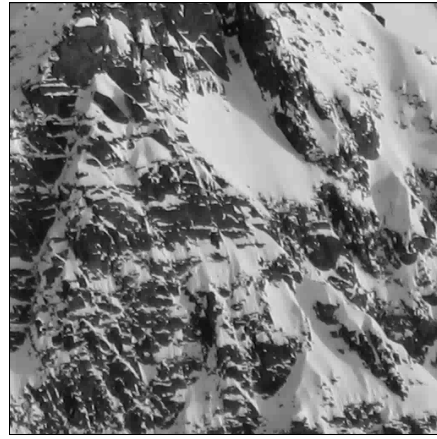
(b) Haar filter
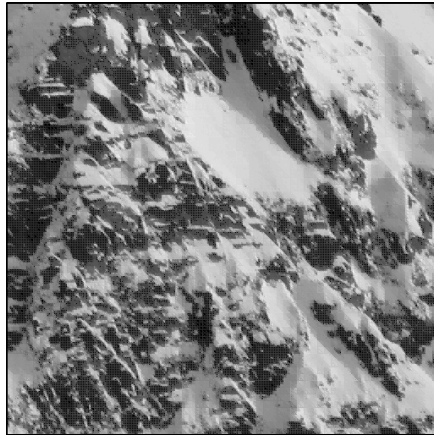
(c) Filter of Example 3.5
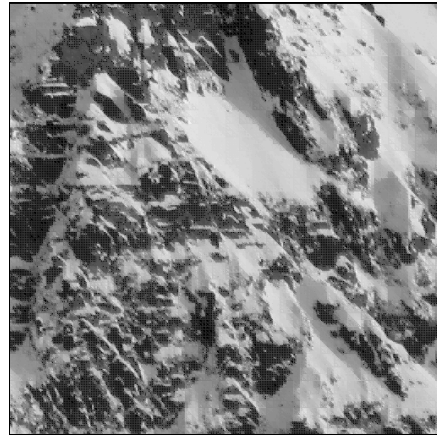
(d) Filter of Example 3.6
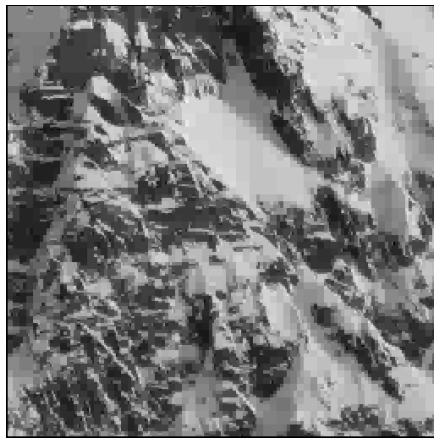
(e) Haar filter
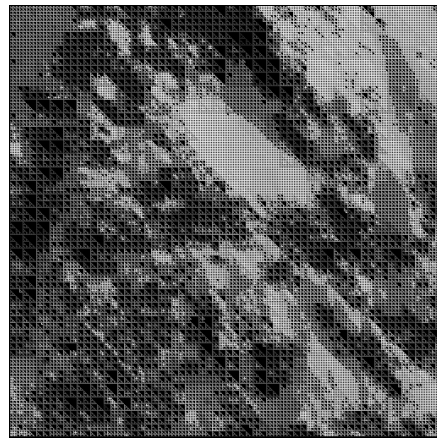
(f) Filter of Example 3.5

FIGURE 8. (a) Original 512×512 grayscale image; (b)-(d) reconstruction using 30% of transform coefficients; (e),(f) using 3% of transform coefficients

where M^* is the adjoint of the filter matrix M defined in the discrete wavelet transform and $\vec{c}$ is a transform coefficient vector of the form,

$$\vec{c} = \begin{pmatrix} a \\ d^1 \\ d^2 \\ d^3 \end{pmatrix}.$$

If $\vec{c}$ contains entries from coefficient sub-matrices at the jth level of decomposition (i.e. from a_j, d_j^1, d_2^2, or d_j^3), then the resulting $\vec{b}$ obtained from the inverse transform will be part of the coefficient sub-matrix a_{j-1}. Image reconstruction is perfect when all of the transform coefficients are kept at all levels. Lossy compression schemes utilize a quantization or thresholding step to remove a certain percentage of transform coefficients as previously described. Figures 7 and 8 show 512×512 grayscale images and reconstructed images using 3% or 30% of the transform coefficients after 9 levels of decomposition.

Note, that for this lossy scheme, the DSGWT doesn't concentrate energy in the transform coefficients of Figure 7 as well as Haar because the structure of the butterfly image isn't well correlated to the structure of the Sierpinski gasket on any level. The result is that the Haar transform outperforms the gasket transform in this task. In particular, upon closer inspection we see that the 'gap' coefficients, those detail coefficients computed from the filter associated with the "gap-filling wavelet" ψ_1, produced by the DSGWT are merely being rearranged from B to d_1^1 in C and from a_j to d_{j+1}^1 at each level of the transform process. This is easily seen in Figures 6c and 6d by noticing that the coefficient sub-matrices d_1^1 and d_2^1 appear to be approximations of the original image. They are, in the sense that they are sampled directly from the upper-right corner of the 2×2 blocks tiling the original image or tiling a_1 respectively. In contrast, the approximation given by the sub-matrices a_1 or a_2 are 'averages' of more than one entry of those same 2×2 blocks. As a result, in the quantization step, when 'gap' coefficients are thrown away they become unrecoverable. This is readily seen in both Figures 7 and 8. Enough transform coefficient information has been lost due to thresholding that 'gap' coefficients have been thrown away and the reconstructed images have 'holes' on those 'gap' supports where there is nothing to reconstruct. The 'gap' information contained in an image matrix is approximately one-third the total image information since it constitutes one-fourth of our transform matrix C at each level of decomposition, thus following a geometric series. Both Figures 7 and 8 throw out more than two-thirds of the transformed information forcing the deletion of unrecoverable 'gap' information as already mentioned. Figure 8 shows a portion of a snow covered mountain with 'gasket' features. At 30%, both the DHWT and DSGWT perform fairly well in this figure, although a bit of bandedness is detectable in the two DSGWT reconstructions. At 3%, weaknesses of both transforms are evident, blockiness in the DHWT reconstruction and noticeable bandedness in the DSGWT reconstruction caused by missing 'gap' coefficients as previously described. Although the large scale structure of the mountain appears amenable to the Sierpinski gasket transform, the mountain does not have the gasket structure at all levels, thus bandedness is still a problem on smaller scales. It is interesting to note, that in the absence of information on the transform side, both the Haar and Sierpinski gasket transforms introduce their structure into the reconstructed images, as demonstrated by Figures 7 and 8. This is to be expected given our discussion of multiresolutions and

the fact that the corresponding basis functions of each transform are the building blocks in the reconstructed images.

5. Conclusion

Very recently, N. Larsen and I. Raeburn have developed an abstract theory relating multi-resolution analyses and directly limit systems of Hilbert spaces constructed from pure isometries. (reference). It is our belief that the fractal wavelets and multi-resolution analyses of Dutkay and Jorgensen can be fit very nicely into this framework, and in future work with Raeburn, the third author hopes to pursue this idea. This Sierpinski gasket case would be a perfect case to which one could apply the abstract theory of direct limits.

In particular, we conjecture that taking the partial isometry S defined on $L^2(\mathbb{T}^2)$ by

$$S(f)(z, w) \ = \ \frac{1}{\sqrt{3}}(1 + z + w)f(2z, 2w),$$

then S is a pure isometry on $L^2(\mathbb{T}^2)$, and forming the direct limit Hilbert space from S via the Larsen-Raeburn construction, one could obtain a multi-resolution analysis and wavelet families isomorphic to the wavelet families described here. It then would be possible to use this direct limit characterization to construct a Fourier transform from $L^2(\mathcal{R}_\mathcal{S}, \mathcal{H})$ to $L^2(\Sigma_2 \times \Sigma_2, \nu)$, corresponding to that constructed by Dutkay in [**Dut**], Corollary 5.8, in the Cantor set case. Here Σ_2 represents the solenoid viewed as the compact Pontryagin dual of the dyadic rationals, and ν is a probability measure on $\Sigma_2 \times \Sigma_2$ determined by the "low-pass" filter mentioned above. We leave this discussion to further research.

References

[BCM02] L. W. Baggett, J. E. Courter, and K. D. Merrill, *The construction of wavelets from generalized conjugate mirror filters in $L^2(\mathbb{R}^n)$*, Appl. Comput. Harmon. Anal. **13** (2002), 201–223.

[BJMP] L.W. Baggett, P.E.T. Jorgensen, K.D. Merrill and J.A. Packer, *Construction of Parseval wavelets from redundant filter systems*, J. Math. Physics, **46**(2005), 083502.

[BLPR] L.W. Baggett, N. Larsen, J. Packer, and I. Raeburn, *Direct limits, MRA's, and Wavelets*, in preparation.

[BMM99] L. W. Baggett, H. A. Medina, and K. D. Merrill, *Generalized multi-resolution analyses and a construction procedure for all wavelet sets in $\mathbb{R}^n$*, J. Fourier Anal. Appl. **5**(1999), 563–573.

[BJ97] O. Bratteli and P.E.T. Jorgensen, *Isometries, shifts, Cuntz algebras and multiresolution wavelet analysis of scale N*, Integral Equations Operator Theory **28**(1997), 382–443.

[Dau] I. Daubechies, *Ten Lectures on Wavelets*, CBMS-NSF Regional Conference Series in Applied Math., vol. 61, SIAM, Philadelphia, 1992.

[Dut] D. Dutkay, *Low-pass filters and reprentations of the Baumslag Solitar group*, Trans. Amer. Math. Soc., to appear.

[DJ] D. Dutkay and P.E.T. Jorgensen, *Wavelets on fractals*, Rev. Math. Iberoamericana, to appear.

[Ed1] G. A. Edgar, *Measure, Topology, and Fractal Geometry*, New York : Springer-Verlag, 1990.

[Ed2] G. A. Edgar, *Integral, Probability, and Fractal Measures*, New York : Springer, 1998.

[GB] R. A. Gopinath, C. S. Burrus, *Wavelet transforms and filter banks*, in "Wavelets: A Tutorial in Theory and Applications", pp. 603–654, C. K. Chui, Ed., Academic Press, Inc., San Diego, CA, 1992.

[Hut] J. E. Hutchinson, *Fractals and self-similarity*, Indiana Univ. Math. J., **30** (1981), 713-747.

[Jor03] P.E.T. Jorgensen, *Matrix factorization, algorithms, and wavelets*, Notices Amer. Math. Soc., to appear.

[LarRae] N. Larsen and I. Raeburn, *From filters to wavelets via direct limits*, Contemp. Math., to appear.

[LPT] L.H. Lim, J.A. Packer, and K. Taylor, *A direct integral decomposition of the wavelet representation*, Proc. Amer. Math. Soc., **129** (2001), 3057-3067.

[Mal99] S.G. Mallat, *A Wavelet Tour of Signal Processing*, 2nd ed., Academic Press, Orlando–San Diego, 1999.

[Mey93] Y. Meyer, *Wavelets and operators*, Different Perspectives on Wavelets (San Antonio, TX, 1993) (Ingrid Daubechies, ed.), Proc. Sympos. Appl. Math., vol. 47, American Mathematical Society, Providence, 1993, pp. 35–58.

[Roy] H. L. Royden, *Real Analysis*, Third Edition, New York: Macmillan Publishing Co., 1988.

[Str] R. S. Strichartz, *Piecewise linear wavelets on Sierpinski gasket type fractals*, J. Fourier Anal. Appl. **3** (1997), 387–416.

DEPARTMENT OF MATHEMATICS, CAMPUS BOX 395, UNIVERSITY OF COLORADO, BOULDER, CO, 80309-0395
    E-mail address: `dandrea@colorado.edu`

DEPARTMENT OF MATHEMATICS, COLORADO COLLEGE, COLORADO SPRINGS, CO 80903-3294
    E-mail address: `kmerrill@coloradocollege.edu`

DEPARTMENT OF MATHEMATICS, CAMPUS BOX 395, UNIVERSITY OF COLORADO, BOULDER, CO, 80309-0395
    E-mail address: `packer@euclid.colorado.edu`